Molecular Pharmacology Fast Forward. Published on November 9, 2007 as doi:10.1124/mol.107.039149

Anandamide Inhibition of 5-HT_{3A} Receptors Varies with Receptor Density and Desensitization

Wei Xiong, Masako Hosoi, Bon-Nyeo Koo and Li Zhang

Laboratory for Integrative Neuroscience, National Institute on Alcohol Abuse and Alcoholism, National Institutes of Health, Bethesda, Maryland 20892, USA

Molecular Pharmacology Fast Forward. Published on November 9, 2007 as DOI: 10.1124/mol.107.039149
This article has not been copyedited and formatted. The final version may differ from this version.

Running Title*:* Anandamide inhibition of 5-HT_{3A} receptors

Address correspondence to:
Dr. Li Zhang
Laboratory for Integrative Neuroscience National Institute on Alcohol Abuse and Alcoholism, National Institutes of Health
5625 Fishers Lane, Bethesda
MD 20892, Tel. 301-443-3755
Fax: 301-480-0466;
Email: lzhang@mail.nih.gov

The number of table: 0
The number of figures: 9
The number of references: 50
The number of words in *Abstract*: 240
The number of words in *Introduction:* 656
The number of words in *Discussion*: 880

ABBREVIATIONS

AEA: anandamide; ANOVA: analysis of variance; DA: dopamine; 5-HT: 5-hydroxytryptophan; GABA: γ-aminobutyric acid; TM: transmembrane domain; VTA: ventral tegmental area; WT: wild type; MCD: mean current density; NOC: nocodazole; AcD: actinomycin; 5-HTID: 5-hydroxyindole; LGIC: ligand-gated ion channel.

Molecular Pharmacology Fast Forward. Published on November 9, 2007 as DOI: 10.1124/mol.107.039149
This article has not been copyedited and formatted. The final version may differ from this version.

Abstract

Converging evidence has suggested that anandamide (AEA), an endogenous agonist of cannabinoid (CB) receptors, can directly interact with certain types of ligand-gated ion channels (LGICs). However, little is known about the molecular and cellular mechanisms of AEA-induced direct effects on LGICs. Here, we report that AEA inhibited the function of serotonin-gated ion channels (5-HT_{3A}) expressed in *Xenopus* oocytes and HEK 293 cells in a manner that was dependent on the steady-state receptor density at the cell surface. The magnitude of AEA inhibition was inversely correlated with the expression levels of receptor protein and function. With increasing surface receptor expression, the magnitude of AEA inhibition decreased. Consistent with this idea, pretreatment with actinomycin D, which inhibits transcription, decreased the amplitude of current activated by maximal concentrations of 5-HT and increased the magnitude of AEA inhibition. AEA did not significantly alter 5-HT_{3A} receptor trafficking. However, AEA accelerated 5-HT_{3A} receptor desensitization time in a concentration-dependent manner without significantly changing receptor activation and deactivation time. The desensitization time was correlated with the AEA-induced inhibiting effect and mean 5-HT current density. Applications of 5-hydroxyindole and nocodazole, a microtubule disruptor, significantly slowed 5-HT_{3A} receptor desensitization and reduced the magnitude of AEA inhibition. These observations suggest that 5-HT_3 receptor density at the steady state regulates receptor desensitization kinetics and the potency of AEA-induced inhibiting effect on the receptors. The inhibition of 5-HT_3 receptors by AEA may contribute to its physiological roles in control of pain and emesis.

Molecular Pharmacology Fast Forward. Published on November 9, 2007 as DOI: 10.1124/mol.107.039149
This article has not been copyedited and formatted. The final version may differ from this version.

Introduction

The endocannabinoid anandamide (AEA) is synthesized from lipid precursors in cell membranes via calcium and G-protein dependent processes. Rapidly released from neurons after membrane depolarization, AEA can modulate many brain functions by preferentially activating presynaptic cannabinoid type 1 (CB1) receptors (Pacher *et al.*, 2006). However, accumulating evidence has indicated that there are additional molecular sites that may mediate AEA action in the central and peripheral nervous system. AEA has also been found to directly modulate the function of various ligand–gated ion channels (LGICs) such as the serotonin type 3 ($5\text{-}HT_3$) receptors, nicotinic acetylcholine (nACh) $\alpha 7$ and $\alpha 4\beta 2$ subunits and glycine receptors (Fan, 1995; Barann *et al.*, 2002; Oz *et al.*, 2002; Oz *et al.*, 2003; Hejazi *et al.*, 2006; Spivak *et al.*, 2007). Moreover, some AEA-induced behavioral effects are not mediated by activation of CB_1 receptors. For example, AEA can induce catalepsy and analgesia in CB1 knockout mice (Zimmer *et al.*, 1999). AEA has been found to attenuate neuronal excitability and pain via a CB1 independent mechanism in mice (Adams *et al.*, 1998).

$5\text{-}HT_3$ receptors are involved in pain transmission, analgesia, mood disorders and drug abuse (Zhang & Lummis, 2006). Selective $5\text{-}HT_3$ receptor antagonists have anxiolytic and antiemetic effects in human and in animal models (Zhang & Lummis, 2006). The levels of $5\text{-}HT_{3A}$ receptors are differentially expressed in brain regions and subpopulations of neurons (Tecott *et al.*, 1993; Morales & Bloom, 1997; Spier *et al.*, 1999; Morales & Wang, 2002). While high levels of $5\text{-}HT_3$ receptors are found in nucleus of the tractus solitarius and area postrema, low levels of the receptors are expressed in nucleus accumbens and striatum (Waeber *et al.*, 1988; Barnes *et al.*, 1989; Waeber *et al.*, 1989;

Molecular Pharmacology Fast Forward. Published on November 9, 2007 as DOI: 10.1124/mol.107.039149
This article has not been copyedited and formatted. The final version may differ from this version.

Pratt *et al.*, 1990; Waeber *et al.*, 1990; Tecott *et al.*, 1993; Morales & Bloom, 1997). Overexpression of 5-HT_{3A} receptors in mouse forebrain increases the sensitivity to alcohol-induced behavioral effects and enhances hippocampal-dependent learning and attention (Engel *et al.*, 1998; Engel & Allan, 1999; Harrell & Allan, 2003). Several naturally occurring polymorphisms in human 5-HT_{3A} receptors can significantly change the levels of receptor expression at cell membrane surfaces (Niesler *et al.*, 2001a; Krzywkowski *et al.*, 2007). These mutations are found to associate with affective disorders, the personality trait of harm avoidance, human face processing and emetogenic sensitivity to anticancer drug-induced side effects such as vomiting and nausea (Niesler *et al.*, 2001a; Niesler *et al.*, 2001b; Melke *et al.*, 2003; Iidaka *et al.*, 2005; Krzywkowski, 2006).

Despite evidence showing that AEA can directly modulate a variety of ion channel functions, the molecular and cellular mechanisms of the AEA-induced CB1 independent effects remain elusive. AEA has been shown to inhibit the 5-HT_{3A} receptor-mediated responses in rat nodose ganglion (NG) neurons and in cell lines expressing mouse and human 5-HT_{3A} subunits (Fan, 1995; Barann *et al.*, 2002; Oz *et al.*, 2002). However, the potency of AEA inhibition has been found to vary significantly among different cell lines. While AEA inhibits 5-HT_3 responses with an EC_{50} value of 0.19 μM in NG neurons, the EC value of AEA inhibition is 3.7 μM in *Xenopus* oocytes expressing homomeric 5-HT_{3A} receptors (Fan, 1995; Oz *et al.*, 2002). This discrepancy is unlikely due to different compositions of the 5-HT_3 subunits that are expressed in native neurons and in heterologous expression systems since the potency of AEA inhibition of homomeric 5-HT_{3A} receptors is similar to that of native receptors expressed in HEK293 cells and NG neurons (Fan, 1995; Barann *et al.*, 2002; Oz *et al.*, 2002). One alternative explanation is that the discrepancy may be due to different levels of receptor expression. To

Molecular Pharmacology Fast Forward. Published on November 9, 2007 as DOI: 10.1124/mol.107.039149
This article has not been copyedited and formatted. The final version may differ from this version.

test this hypothesis, we examined the relationships between the extent of the AEA inhibition of 5-HT_{3A} receptors and receptor density at the cell surface. Our results suggest that the steady state density of 5-HT_3 receptors critically influences on receptor desensitization and the sensitivity of 5-HT_3 receptors to AEA-induced inhibiting effect.

Molecular Pharmacology Fast Forward. Published on November 9, 2007 as DOI: 10.1124/mol.107.039149
This article has not been copyedited and formatted. The final version may differ from this version.

Materials and Methods

Preparation of cRNAs and Expression of Receptors. The cDNA clone of the mouse 5-HT_{3A} subunit was provided by Dr. David Julius (University of California, San Francisco, CA). The cDNA clone of the human 5-HT_{3A} subunit was purchased from OriGen, Inc (Rockville, MD). Complementary RNAs (cRNAs) were synthesized in vitro using a mMessage mMACHINE RNA transcription kit (Ambion Inc., Austin, TX). The quality and sizes of synthesized cRNAs were confirmed by denatured RNA agarose gels. Mature female *Xenopus* laevis frogs were anesthetized by submersion in 0.2% 3-aminobenzoic acid ethyl ester (Sigma, St Louis MO). Oocytes were surgically excised and separated. The follicular cell layer of the oocytes was removed by treatment with type A collagenase (Sigma-Aldrich) for 10 min at room temperature. Although the amount of cRNA injected into oocytes varied from 1 to 100 ng, as indicated, the injection volume of diethylpyrocarbonate (DEPC)-treated water was kept in 20 nl throughout the entire experiment. Oocytes were incubated at 19 °C in modified Barth's solution (MBS): 88 mM NaCl, 1 mM KCl, 2.4 mM $NaHCO_3$, 2.0 mM $CaCl_2$, 0.8 mM $MgSO_4$, 10 mM HEPES, pH7.4.

***Xenopus* Oocyte Electrophysiological Recording**. After incubation for 2-5 days, oocytes were studied at room temperature (20-22 °C) in a 90 μl chamber. The oocytes were superfused with MBS at a rate of 6 ml/min. Agonists and chemical agents were diluted in the bath solution and applied to the oocytes for a specified time, using a solenoid valve-controlled superfusion system. Membrane currents were recorded by two-electrode voltage-clamp at a holding potential of –70 mV, using a Gene Clamp 500 amplifier (Axon Instruments Inc., Burlingame, CA). The recording microelectrodes were filled with 3 M KCl and had electrical resistances of 0.5-3.0 MΩ. Data were acquired using pClamp 9.1 software (Axon). Average values are expressed as means ± S.E.

Molecular Pharmacology Fast Forward. Published on November 9, 2007 as DOI: 10.1124/mol.107.039149
This article has not been copyedited and formatted. The final version may differ from this version.

Western Blot of Membrane Surface Proteins. Immediately after treatment with AEA, *Xenopus* oocytes expressing 5-HT_{3A} receptors were washed in PBS and incubated with *N*-hydroxysuccinimide-SS-biotin (NHS-SS-biotin; Pierce) at a concentration of 1.5 mg/ml in phosphate-buffer saline (PBS) for 30 min at 4°C under nonpermeabilizing conditions, as described previously (Hollmann *et al.*, 1994; Lan *et al.*, 2001). The oocytes were then washed and homogenized. The homogenate was centrifuged repeatedly at 1,000 *g* for 10 min at 4°C until all yolk granules and melanosomes were pelleted. The final supernatant was incubated with 100 µl neutravidin-linked beads (Pierce) by end-over-end rotation for 2 hr at 4°C. The beads were centrifuged and washed extensively to isolate bead-bound proteins. Labeled proteins were eluted from the beads by dithiothreitol (DTT)-containing SDS-PAGE loading buffer and loaded onto 10% SDS/PAGE. After transfer onto a PVDF membrane (Invitrogen), the surface proteins were blocked with PBS (pH 7.5) containing 0.1% Tween-20 (Sigma) and 5% nonfat powdered milk and then incubated for 1 hr with a polyclonal antibody (pAb120, 1:2,000) directed to the extracellular N-terminal domain of the 5-HT_{3A} receptor (Spier & Lummis, 1997). The proteins were washed, blotted with a 1:600 dilution of fluorescein-linked anti-rabbit Ig in PBS and incubated with anti-fluorescein-AP conjugate (Pierce) at 1:2500 dilution in PBS for 1 hour. The proteins detected by ECF substrate (Amersham) were scanned using a Molecular Dynamics Storm Gel and Blot Imaging System with ImageQuant Image Analysis Software (Amersham).

HEK 293 cell transfection and whole cell recording. HEK 293 cells were cultured as described previously (Hu *et al.*, 2006). The plasmid cDNA of human 5-HT_{3A} receptors was transfected with

Molecular Pharmacology Fast Forward. Published on November 9, 2007 as DOI: 10.1124/mol.107.039149
This article has not been copyedited and formatted. The final version may differ from this version.

SuperFect Transfection kit (Qiagen, Hidden, CA). The currents were recorded 24-48 hr after transfection. Cells were lifted and continuously superfused with a solution containing 140 mM NaCl, 5 mM KCl, 1.8 mM $CaCl_2$, 1.2 mM $MgCl_2$, 5 mM glucose, and 10 mM HEPES (pH 7.4 with NaOH; ~340 mosmol with sucrose). Membrane currents were recorded in the whole-cell configuration using an Axopatch 200B amplifier (Axon) at 20-22°C. Cells were held at –60 mV unless otherwise indicated. Data were acquired using pCLAMP 9 software (Molecular Devices, Sunnyvale, CA). Bath solutions were applied through 3 barrel square glass tubing (Warner Instrument, Hamden, CT) that had been pulled to a tip diameter of ~200 μm. Drugs were applied through Warner fast-step stepper-motor driven system. The 10-90% rise time of the junction potential at whole-cell recording was 4-12 ms.

Staining and imaging of 5-HT_{3A} receptor α-bungarotoxin (BTX)-Tag transfected in HEK 293 cells. To generate 5-HT_{3A} receptor-BTX-tag, two copies of the sequence 5'-TGGCGGTAC-TACGAGAGCAGCCTGGAGCCCTACCCCGAC-3' were inserted into both 5' and 3' ends of the 5-HT_{3A} subunit subcloned in pCDNA 3.1 (-) using PCR amplification. The 5-HT_{3A}-BTX-tag was transfected into HEK 293 cells using Lipofectamine 2000 (Invitrogen, Carlsbad, CA). 24-48 hrs after transfection, living cells were stained with tetramethylrhodamine-BTX at 1 μg/ml (Molecular Probes, Eugene, OR) for 5 min at room temperature. Cells were washed twice with PBS and then incubated with 2 μM AEA for 5 min. Cells were stained with Alexa Fluor 488-BTX at 1 μg/ml for 5 min, washed and fixed with 4% paraformaldehyde. Cells were rinsed with PBS and mounted in a glycerol-based mounting medium. Cells were imaged with a CCD camera attached to a Zeiss Axiovert epifluorescence microscope. The Alexa-488 was excited at 480/35 nm and the emission of light was

Molecular Pharmacology Fast Forward. Published on November 9, 2007 as DOI: 10.1124/mol.107.039149
This article has not been copyedited and formatted. The final version may differ from this version.

colleted using a 533/35 emission filter with a 1.3 NA 100X objective. The tetramethylrhodamine was excited at 540/25 nm and the emission of light was collected using a 605/55 emission filter.

Data Analysis. Statistical analysis of concentration-response data was performed with the use of the nonlinear curve-fitting program Prism. Data were fit using the Hill equation

$$I/I_{max} = 1/[1 + (EC_{50}/[\text{Agonist}])^{nH}] \quad (1)$$

where I is the current amplitude activated by a given concentration of agonist ([Agonist]), I_{max} is the maximum response of the cell, nH is the Hill coefficient and EC_{50} is the concentration eliciting a half-maximal response. Data were statistically compared by the paired *t*-test, or analysis of variance (ANOVA), as noted. Average values are expressed as mean ± standard error (SE).

Kinetic Ananlysis. Receptor activation rate was induced by 30 μM 5-HT and estimated by measuring the slope of the initial inward component of current between 10 and 30% of the maximal current (10-30% rise time). Receptor desensitization was induced by prolonging incubation with AEA for 30 s. The deactivation time was recorded for 30 s immediately following a brief application of 1 mM 5-HT for 5 ms. The time constants of deactivation and desensitization were determined by fitting with exponential functions using the Marquardt-Levenberg algorithm in Clampfit. The deactivation and desensitization time constants for 5-HT_3-mediated currents were best fit using a bi-exponential function when expressed in HEK 293 cells. However, a single exponential function was sufficient to accurately fit the desensitization decays of current activated by 5-HT in the presence of AEA. In this case, fast and slow components were normalized from two components to single component following

Molecular Pharmacology Fast Forward. Published on November 9, 2007 as DOI: 10.1124/mol.107.039149
This article has not been copyedited and formatted. The final version may differ from this version.

the equation:

$(A_{FAST}*\tau_{FAST} + A_{SLOW}*\tau_{SLOW})$ (2)

where as τ_{FAST} and τ_{SLOW} were the fast and slow decay time constants, and A_{FAST} and A_{SLOW} were the relative proportion of the fast and slow components.

Chemicals. All chemicals used in preparing the solutions were from Sigma-Aldrich (St. Louis, MO). 5-HT was applied by gravity flow via a micropipette positioned 3 mm from the oocyte. Stock solutions of AEA, 5-hydroxyindole (5-HTID) and nocodazole (NOC) were prepared in dimethylsulfoxide (DMSO) at a concentration of 10 mM. DMSO alone did not affect 5-HT receptor-mediated current when added at concentrations up 0.2 % (v/v), which was twice as high as the most concentrated DMSO used in our experiments.

Molecular Pharmacology Fast Forward. Published on November 9, 2007 as DOI: 10.1124/mol.107.039149
This article has not been copyedited and formatted. The final version may differ from this version.

Results

AEA inhibition is independent of agonist concentrations. Consistent with a previous observation (Oz *et al.*, 2002), incubation of AEA (10 μM) for 10-20 min produced gradually developing inhibition of 5-HT (1 μM)-induced currents in *Xenopus* oocytes previously injected with 2.5 ng of the mouse 5-HT_{3A} subunit cRNA (Fig. 1A). The AEA-induced inhibition reached a maximum of 86% after a 10 min exposure and was completely reversed 30 min after discontinuation of drug application (Fig. 2B). The inhibition by AEA was concentration-dependent with an EC_{50} value of 239 ±13 nM and slope value of 0.8 ± 0.16 (Fig. 1C). The effect of 10 μM AEA on 5-HT_{3A} receptors was also studied in the presence of different concentrations of 5-HT. The inhibition by AEA was equipotent at all agonist concentrations (Fig. 1D). The EC_{50} and slope values of the 5-HT-concentration response curves were 1.6 ± 0.05 μM and 1.5 ± 0.2 in the absence of AEA, and 1.9 ± 0.2 μM and 1.8 ± 1.0 in the presence of 10 μM AEA. These values were not significantly different ($p > 0.2$, unpaired t test, n = 5).

AEA inhibition correlates with receptor surface protein and function. To examine if the AEA inhibition depends on surface receptor density, we injected various concentrations (1, 2.5, 10, 25, 50 and 75 ng) of mouse 5-HT_{3A} subunit cRNA into *Xenopus* oocytes. We first measured the surface expression of 5-HT_{3A} receptors in oocytes using Western blots by labeling cell-surface proteins with sulfo-NHS-SS-biotin (Lan *et al.*, 2001). Fig. 2A reveals a representative Western blot of surface receptor proteins from cells injected with 50, 10 and 1 ng of 5-HT_{3A} receptor cRNA. The amplitude of current activated by 100 μM 5-HT also increased with increasing cRNA injection levels (Fig. 2B). AEA at 10 μM inhibited 5-HT_{3A} receptor-mediated current in a manner

Molecular Pharmacology Fast Forward. Published on November 9, 2007 as DOI: 10.1124/mol.107.039149
This article has not been copyedited and formatted. The final version may differ from this version.

that depended on the expression levels of surface receptor protein (Fig. 2B, C). The magnitude of AEA inhibition was strongest at lower receptor expression levels. For instance, the maximal AEA inhibition was 95% (5 ± 2 % of control) in oocytes injected with 2.5 ng of 5-HT_{3A} receptor cRNA, whereas the maximal inhibition was only 25% (75 ± 6 % of control) in oocytes injected with 50 ng of 5-HT_{3A} receptor cRNA. These values were significantly different (Fig. 2C; unpaired t test, $p < 0.001$). The EC_{50} values of AEA inhibition differed by nearly 120-fold between oocytes previously injected with 1 and 50 ng of cRNAs (Fig. 2D). For instance, the EC_{50} value for AEA inhibition was 167 ± 12 nM in cells injected with 1 ng of cRNA, whereas the EC_{50} value for AEA inhibition was 20 ± 2 μM in cells injected with 50 ng of cRNA. These values were significantly different (Fig. 2D; $p < 0.001$, unpaired t test, n = 5). The magnitude of inhibition produced by 10 μM AEA was strongly correlated with the amount of the cRNA injected into the oocytes (Fig. 3A, $p < 0.0001$), the expression level of the receptor proteins (Fig. 3B, $p < 0.0001$) and the maximal current activated by 100 μM 5-HT (Fig. 3C; $p = 0.002$).

Actinomycin D (AcD) increases AEA inhibition. To further confirm the relationship between receptor density and AEA inhibition, we preincubated oocytes with 10 μg/ml AcD, which inhibits RNA transcription, for 24 hrs prior to recordings. We observed that AcD significantly reduced current amplitude activated by 100 μM 5-HT from 7.8 ± 2.5 μA to 1.4 ±0.4 μA (Fig. 4A, $p < 0.001$, unpaired t test, n = 7). This suggests that AcD can reduce the functional expression of 5-HT_{3A} receptors. On the other hand, AcD significantly increased the magnitude of AEA inhibition from 53 ± 11 % to 88 ± 2 % (Fig. 4B; $p < 0.02$, unpaired t test, n = 7).

Molecular Pharmacology Fast Forward. Published on November 9, 2007 as DOI: 10.1124/mol.107.039149
This article has not been copyedited and formatted. The final version may differ from this version.

AEA inhibition correlates with mean current density. The above observations indicate that potency of AEA inhibition of 5-HT_{3A} receptor function depends on receptor steady state density at the cell surface. However, one can argue if this phenomenon occurs exclusively in *Xenopus* oocytes where a slow perfusion system is used. To answer this question, we performed whole-cell recordings combined with fast drug perfusion to examine the effect of AEA on the 5-HT_{3A} subunits expressed in HEK 293 cells. In cells transiently expressing 5-HT_{3A} receptors, the amplitude of current activated by maximal 5-HT (100 μM) varied from 0.3 to 7.9 nA, indicating that the levels of receptor expression differ substantially at the surface of individual cells. AEA inhibited current amplitude activated by 30 μM 5-HT. The magnitudes of average percent inhibition by 0.1 and 1 μM AEA were 58 ± 3 % and 92 ± 2 %. These data are in line with a previous study (Barann *et al.*, 2000). Similar to the observations in oocyte experiments, HEK cells that exhibited relatively low current amplitudes were more sensitive to AEA than those that exhibited high current amplitudes (Fig. 5A). We then calculated mean current density (MCD) by plotting maximal 5-HT-current amplitude over capacitance of each individual cell. The extent of MCD was inversely correlated with the percent AEA inhibition of current peak (Fig. 5B; linear regression, $p < 0.01$, n = 13) and current area (Fig. 5C; linear regression, $p < 0.01$, n = 13).

AEA does not affect 5-HT_{3A} receptor trafficking. The AEA inhibition develops slowly and requires a preincubation of AEA to reach the maximal effect. This observation promotes us to ask whether or not AEA inhibits 5-HT_3 receptors by modulating receptor internalization. We first examined the effect of AEA on 5-HT_{3A} receptor trafficking in living HEK 293 cells that express 5-HT_{3A} receptor proteins tagged on the extracellular N- and carboxyl--terminus with a α-

Molecular Pharmacology Fast Forward. Published on November 9, 2007 as DOI: 10.1124/mol.107.039149
This article has not been copyedited and formatted. The final version may differ from this version.

bungarotoxin pharmatope (BTX). The 13 amino acid BTX pharmatope is derived from the nACh receptor. The BTX pharmatope-tagged receptors can be labeled by BTX, which allows us to specifically label surface receptors and to visualize receptor trafficking in living cells. Cells were labeled with tetramethylrhodamine-BTX (*red*) prior to exposure to AEA and then treated with 2 μM AEA for 5 min. These cells were then labeled with Alexa-488-BTX (*green*). Under this experimental procedure, receptors that were endocytosed during AEA incubation period were observed as red signal within interior of cells. Those Alexa-488 labeled-receptors that did not enter endocytosis were double-labeled and appeared as yellow signal surround cell perimeter; whereas those appear as green may represent newly inserted channels. Fig. 6A illustrates double-labeling of 5-HT_{3A} receptors without and with 2 μM AEA. The majority of the 5-HT_{3A} receptors that were on the cells surface during initial period had been endocytosed in the absence and presence of AEA. Next, we used protein biotinylation-labeling method to quantitatively evaluate surface expression of 5-HT_{3A} receptor proteins. The density of the surface protein revealed by Western blot appeared to be similar before and 5, 10 and 20 min after AEA (Fig. 6B). The average values of protein gel intensity measured were 97 ± 10%, 110 ± 14% and 104 ± 12% of control (Fig. 6C). There values were not significantly different (Fig. 6C; $p > 0.5$, ANOVA).

AEA accelerates receptor desensitization. To explore the mechanisms that underlie AEA inhibition of 5-HT_{3A} receptors, we conducted kinetic analysis using fast drug perfusion. While AEA did not significantly alter the 10-30% rise time of 5-HT-activated currents (2.9 ± 0.1 ms vs. 3.1 ± 0.1 ms, unpaired t test, $p = 0.2$), AEA appeared to accelerate the desensitization decay of 5-HT-activated current (Fig. 7A) in the prolonged presence of 5-HT ("desensitization"). To properly

Molecular Pharmacology Fast Forward. Published on November 9, 2007 as DOI: 10.1124/mol.107.039149
This article has not been copyedited and formatted. The final version may differ from this version.

evaluate the desensitization kinetics, we normalized the fast and slow components using the weighted sum formula described in 'Materials and Methods'. We first examined the effect of AEA on the time courses of 5-HTactivated current (*solid circles*) and receptor desensitization (*open circles*). Both AEA-induced inhibition and desensitization developed in similar time courses. However, the receptor desensitization reached the maximal extent after preincubation of AEA for 2 min, whereas the maximal extent of AEA inhibition required 5 min (Fig. 7B). The weighted sum of the desensitization time constant components for 5-HT alone was 536 ± 87 ms, whereas the weighted sum of the desensitization time constants in the presence of 0.03 μM and 0.1 μM AEA were 386 ± 68 ms, 76 ± 17 ms. These values were significantly different from that of control (Fig. 7C, $p < 0.01$, ANOVA). In contrast, AEA did not significantly affect the deactivation time course, which was also best fit by a bi-exponential function. The deactivation time constants of the fast decay component averaged 0.12 ± 0.01 s and 0.13 ± 0.01 s with and without AEA, respectively. The deactivation time constants of the slow component averaged 1.9 ± 0.1 s and 1.6 ± 0.2 s in the absence and presence of AEA, respectively. These values were not significantly different ($p > 0.2$, unpaired t test, n = 12). A previous study showed that AEA bound to bovine serum albumin (BSA) (Bojesen & Hansen, 2003). A recent study has reported that BSA can accelerate the recovery time of AEA inhibition of nAChα4β2 subunits (Spivak *et al.*, 2007). In view of these findings, we applied 0.3% of BSA during washout time of AEA-induced inhibition. We observed that BSA accelerated the recovery time after AEA inhibition. For instance, the average recovery rates of $I_{5\text{-HT}}$ after AEA inhibition were 42 ± 3% and 59 ± 6% of control current without and with BSA 2 min after AEA application. These values were significant different ($p< 0.01$, unpaired t test, n = 6).

Molecular Pharmacology Fast Forward. Published on November 9, 2007 as DOI: 10.1124/mol.107.039149
This article has not been copyedited and formatted. The final version may differ from this version.

Receptor desensitization correlates with MCD. The above observations suggest that AEA accelerates receptor desensitization. Given the observation that MCD was correlated with AEA inhibition, we predicted that MCD would also correlate with receptor desensitization. It was proved to be the case as a strong correlation was observed between receptor density (MCD) and desensitization time (Fig. 8A; linear regression, $p < 0.001$). MCD was also correlated with percent inhibition by AEA (Fig. 8B; linear regression, $p < 0.001$, n = 15). However, no significant correlation was observed between receptor activation/deactivation and MCD (Fig. 8C,D; $p > 0.5$, n = 15).

5-hydroxyindole (5-HTID) and nocodazole (NOC) slow receptor desensitization and reduce AEA-induced inhibiting effect on 5-H_{3A} receptors. To further explore the mechanism of AEA inhibition, we designed the following experiments. First, we pretreated cells with 25 μM NOC, a microtubule disruptor, for 4 hrs prior to electrophysiological recording of 5-HT-activated current. A recent study from our laboratory has shown that disruption of microtubule by NOC can significantly slow mouse 5-HT_3 receptor desensitization (Emerit *et al.*, 2005). Consistent with this study, NOC treatment slowed the decay of 5-HT-activated current in HEK 293 cells expressing human 5-HT_{3A} receptors (Fig. 9A). Another approach we used was 5-HTID, which has been shown to slow 5-HT_3 receptor desensitization (van Hooft *et al.*, 1997; Gunthorpe & Lummis, 1999). Simutanously application 5-HTID at 5 mM with 5-HT slowed the decay of 5-HT-activated current (Fig. 9A). Pretreatment of HEK 293 cells with NOC and 5-HTID slowed 5-HT_{3A} receptor desensitization time by ~6-fold (*solid bars*) and, on the other hand, significantly reduced the

Molecular Pharmacology Fast Forward. Published on November 9, 2007 as DOI: 10.1124/mol.107.039149
This article has not been copyedited and formatted. The final version may differ from this version.

average percentage of AEA inhibition from 54 ± 3 % (control) to 33 ± 2% and 27 ± 6% (Fig. 9B; *open bars*). These values were significantly different ($p < 0.01$, ANOVA, n = 11). The mean current densities (MCD) induced by maximal concentration of 5-HT were 0.22 ± 0.04 nA/pF, 0.26 ± 0.05 nA/pF and 0.18 ± 0.04 nA/pF in the absence (control) and presence of NOC and 5-HTID (Fig. 9C). These values were not significantly different (ANOVA, $p > 0.2$, n=14-22).

Molecular Pharmacology Fast Forward. Published on November 9, 2007 as DOI: 10.1124/mol.107.039149
This article has not been copyedited and formatted. The final version may differ from this version.

Discussion

Our data presented in this study indicate that the sensitivity of 5-HT_3 receptors to AEA-induced inhibiting effect depends on steady state receptor density at the cell surface. We have shown that surface protein and functional expression of the 5-HT_{3A} receptors were correlated with the extent of AEA inhibition in *Xenopus* oocyte and HEK 293 cells expressing 5-HT_{3A} receptors. A reduction in the functional expression of 5-HT_{3A} receptors induced by AcD treatment increased the sensitivity of 5-HT_{3A} receptors to AEA-induced inhibition. It should be noted that the correlation observed in *Xenopus* oocytes was more dramatic than that of HEK 293 cells. This difference is due to fact that the expression levels of 5-HT_{3A} receptor protein can be readily manipulated in *Xenopus* oocytes. For instance, we injected oocytes with various concentrations of cRNA over a range from 1ng to 75 ng. As a result, we observed a difference in the maximal current amplitudes by nearly 350-fold (200 nA to 7000 nA). However, the difference of the maximal current amplitude was only 10-fold (200 pA-7000 pA) in HEK 293 cells transiently transfected with 5-HT_{3A} receptor cDNA.

Our results also suggest that receptor density contributes to receptor desensitization, which is the key factor determining the sensitivity of 5-HT_{3A} receptors to AEA-induced inhibition. This is evidenced by our observation that both NCD and 5-HTID reduced both receptor desensitization and AEA inhibition without significantly changing maximal 5-HT current amplitude. We propose that the low density 5-HT_{3A} receptors at the cell surface should be more efficient than the high density receptors to enter the desensitized state when exposed to agonist or agonist plus AEA. This idea is supported by a recent study from our laboratory that 5-HT_{3A} receptor desensitization is regulated by the light chain of the microtubule-associated protein 1B (LC1) (Emerit *et al.*, 2005). In this case,

Molecular Pharmacology Fast Forward. Published on November 9, 2007 as DOI: 10.1124/mol.107.039149
This article has not been copyedited and formatted. The final version may differ from this version.

MAP1B-LC1 reduces steady state receptor density at the cell surface and accelerates receptor desensitization kinetics at the steady-state. Consistent with our hypothesis, the steady state density of $GABA_A$ receptors at the cell surfaces has also been found to critically regulate receptor desensitization (Chen *et al.*, 2000; Petrini *et al.*, 2003; Boileau *et al.*, 2005). Similarly, there is a study showing that desensitization of glycine receptors varies with receptor density (Legendre *et al.*, 2002). It should be pointed out that except receptor density there are many other factors contributable to receptor desensitization. These physiological modulators include external calcium concentration (Hu & Lovinger, 2005), posttranslational modification of the receptor protein (Yakel & Jackson, 1988)and subunit composition (Hapfelmeier *et al.*, 2003). Future experiments are awaited to determine how the factors listed above regulate AEA-induced inhibiting effect on 5-HT_3 receptors.

AEA appears to selectively alter 5-HT_{3A} receptor desensitization kinetics without changing activation and deactivation kinetic properties. This observation is consistent with a previous study showing that AEA did not alter the specific binding of the 5-HT_3 receptor antagonist [^{3}H]-GR65630 in HEK 293 cells expressing 5-HT_{3A} receptors (Barann *et al.*, 2002). AEA belongs to a group of signaling lipids, which can bind proteins through a hydrogen-bonding like interaction (Bojesen & Hansen, 2003). It is plausible to predict that AEA reduces current amplitude by lowering the energy barrier for receptors to enter a desensitized state. Conversely, 5-HT_{3A} receptor density at the steady state contributes to the free energy barrier required for conformational changes during a receptor desensitization process. It should be pointed out that AEA is unlikely to be an open channel blocker (OCB) at 5-HT_3 receptors for the following reasons. First, the inhibitory effect of AEA on 5-HT_{3A} receptors was not voltage-dependent (Fan, 1995; Oz *et al.*, 2002). Second, AEA accelerated receptor

Molecular Pharmacology Fast Forward. Published on November 9, 2007 as DOI: 10.1124/mol.107.039149
This article has not been copyedited and formatted. The final version may differ from this version.

desensitization in a concentration dependent manner, whereas a typical OCB usually slows receptor desensitization with increasing its concentrations. Third, AEA became less potent to inhibit 5-HT_{3A} receptors when receptor desensitization was slowed after NOC and 5-HTID treatment, whereas an OCB should be more potent to act at a receptor when its desensitization slows.

LGICs constantly move in and out of synaptic membrane surfaces under various physiological and pathological conditions (Moss & Smart, 2001). Such dynamic receptor trafficking is essential for synaptic transmission and plasticity (Sheng & Pak, 2000). Multiple factors can contribute to the regulation of receptor density at synaptic membrane surfaces. Expression levels of 5-HT_{3A} receptors can be mediated through mechanisms that involve activation of protein kinases (Sun *et al.*, 2003), cytoskeleton proteins (Emerit *et al.*, 2005), naturally occurring genetic variants (Niesler *et al.*, 2001a) and abused drugs such as alcohol (Ciccocioppo *et al.*, 1998). In addition, the expression of these receptors is increased in serotonin transporter deficient mice, suggesting that the extracellular concentration of 5-HT may also influence receptor density (Mossner *et al.*, 2004). In addition to psychotropic effects, cannabinoids and endocannabinoids also exert strong antinociceptive and antiemetic effects (Pacher *et al.*, 2006). Coincidently, selective 5-HT_3 receptor antagonists are also known to effectively control pain and emesis (Zhang & Lummis, 2006). It should be interesting for future studies to determine the physiological and therapeutic significance of AEA inhibition of 5-HT_3 receptors in human and animal models.

Collectively, we conclude that 5-HT_3 receptor steady-state density determines receptor desensitization kinetics and the sensitivity of the receptor to the inhibitory effect of AEA. Such a

Molecular Pharmacology Fast Forward. Published on November 9, 2007 as DOI: 10.1124/mol.107.039149
This article has not been copyedited and formatted. The final version may differ from this version.

mechanism appears to account for the variability in AEA inhibition of 5-HT_3 receptors expressed in different neurons and cell lines. This mechanism could also be applicable to the inhibitory effect of AEA on the other members of LGICs such as nACh and glycine receptors since AEA has been found to accelerate receptor desensitization kinetics in a manner similar to that observed in 5-HT_3 receptors (Lozovaya *et al.*, 2005; Spivak *et al.*, 2007).

FOOTNOTES

This work was supported by funds from the intramural program of National Institute on Alcohol Abuse and Alcoholism.

Acknowledgements

We thank Drs. David Julius and Sarah S.C. Lummis for kindly providing the cDNA clones of mouse 5-HT_3 receptor and polyclonal 5-HT_{3A} receptor antiserum. We thank Dr. David M. Lovinger for comments on this manuscript. We also thank Ms. Guoxiang Lou for constructing 5-HT_{3A}R-BTX

Molecular Pharmacology Fast Forward. Published on November 9, 2007 as DOI: 10.1124/mol.107.039149
This article has not been copyedited and formatted. The final version may differ from this version.

References

Adams IB, Compton DR & Martin BR. (1998). Assessment of anandamide interaction with the cannabinoid brain receptor: SR 141716A antagonism studies in mice and autoradiographic analysis of receptor binding in rat brain. *J Pharmacol Exp Ther* **284,** 1209-1217.

Barann M, Meder W, Dorner Z, Bruss M, Bonisch H, Gothert M & Urban BW. (2000). Recombinant human 5-HT3A receptors in outside-out patches of HEK 293 cells: basic properties and barbiturate effects. *Naunyn Schmiedebergs Arch Pharmacol* **362,** 255-265.

Barann M, Molderings G, Bruss M, Bonisch H, Urban BW & Gothert M. (2002). Direct inhibition by cannabinoids of human 5-HT3A receptors: probable involvement of an allosteric modulatory site. *Br J Pharmacol* **137,** 589-596.

Barnes JM, Barnes NM, Costall B, Ironside JW & Naylor RJ. (1989). Identification and characterisation of 5-hydroxytryptamine 3 recognition sites in human brain tissue. *J Neurochem* **53,** 1787-1793.

Boileau AJ, Pearce RA & Czajkowski C. (2005). Tandem subunits effectively constrain GABAA receptor stoichiometry and recapitulate receptor kinetics but are insensitive to GABAA receptor-associated protein. *J Neurosci* **25,** 11219-11230.

Bojesen IN & Hansen HS. (2003). Binding of anandamide to bovine serum albumin. *J Lipid Res* **44,** 1790-1794.

Chen L, Wang H, Vicini S & Olsen RW. (2000). The gamma-aminobutyric acid type A (GABAA) receptor-associated protein (GABARAP) promotes GABAA receptor clustering and modulates the channel kinetics. *Proc Natl Acad Sci U S A* **97,** 11557-11562.

Ciccocioppo R, Ge J, Barnes NM & Cooper SJ. (1998). Central 5-HT3 receptors in P and in AA alcohol-preferring rats: An autoradiographic study. *Brain Res Bull* **46,** 311-315.

Emerit MB, Sun H, Hu X-Q, Schoenebeck JC, Peoples RW, Miko A, Williams CK & L. Z. (2005). 5-HT3 receptor linkage to cytoskeleton by MAP1B determines receptor desensitization kinetics. *Abst Soc Neurosci***,** 844.817.

Engel SR & Allan AM. (1999). 5-HT3 receptor over-expression enhances ethanol sensitivity in mice. *Psychopharmacology (Berl)* **144,** 411-415.

Engel SR, Lyons CR & Allan AM. (1998). 5-HT3 receptor over-expression decreases ethanol self administration in transgenic mice. *Psychopharmacology (Berl)* **140,** 243-248.

Fan P. (1995). Cannabinoid agonists inhibit the activation of 5-HT3 receptors in rat nodose

ganglion neurons. *J Neurophysiol* **73,** 907-910.

Gunthorpe MJ & Lummis SC. (1999). Diltiazem causes open channel block of recombinant 5-HT3 receptors. *J Physiol* **519 Pt 3,** 713-722.

Hapfelmeier G, Tredt C, Haseneder R, Zieglgansberger W, Eisensamer B, Rupprecht R & Rammes G. (2003). Co-expression of the 5-HT3B serotonin receptor subunit alters the biophysics of the 5-HT3 receptor. *Biophys J* **84,** 1720-1733.

Harrell AV & Allan AM. (2003). Improvements in hippocampal-dependent learning and decremental attention in 5-HT(3) receptor overexpressing mice. *Learn Mem* **10,** 410-419.

Hejazi N, Zhou C, Oz M, Sun H, Ye JH & Zhang L. (2006). Delta9-tetrahydrocannabinol and endogenous cannabinoid anandamide directly potentiate the function of glycine receptors. *Mol Pharmacol* **69,** 991-997.

Hollmann M, Maron C & Heinemann S. (1994). N-glycosylation site tagging suggests a three transmembrane domain topology for the glutamate receptor GluR1. *Neuron* **13,** 1331-1343.

Hu XQ & Lovinger DM. (2005). Role of aspartate 298 in mouse 5-HT3A receptor gating and modulation by extracellular Ca2+. *J Physiol* **568,** 381-396.

Hu XQ, Sun H, Peoples RW, Hong R & Zhang L. (2006). An interaction involving an arginine residue in the cytoplasmic domain of the 5-HT3A receptor contributes to receptor desensitization mechanism. *J Biol Chem* **281,** 21781-21788.

Iidaka T, Ozaki N, Matsumoto A, Nogawa J, Kinoshita Y, Suzuki T, Iwata N, Yamamoto Y, Okada T & Sadato N. (2005). A variant C178T in the regulatory region of the serotonin receptor gene HTR3A modulates neural activation in the human amygdala. *J Neurosci* **25,** 6460-6466.

Krzywkowski K. (2006). Do polymorphisms in the human 5-HT3 genes contribute to pathological phenotypes? *Biochem Soc Trans* **34,** 872-876.

Krzywkowski K, Jensen AA, Connolly CN & Brauner-Osborne H. (2007). Naturally occurring variations in the human 5-HT3A gene profoundly impact 5-HT3 receptor function and expression. *Pharmacogenet Genomics* **17,** 255-266.

Lan JY, Skeberdis VA, Jover T, Grooms SY, Lin Y, Araneda RC, Zheng X, Bennett MV & Zukin RS. (2001). Protein kinase C modulates NMDA receptor trafficking and gating. *Nat Neurosci* **4,** 382-390.

Legendre P, Muller E, Badiu CI, Meier J, Vannier C & Triller A. (2002). Desensitization of

homomeric alpha1 glycine receptor increases with receptor density. *Mol Pharmacol* **62,** 817-827.

Lozovaya N, Yatsenko N, Beketov A, Tsintsadze T & Burnashev N. (2005). Glycine receptors in CNS neurons as a target for nonretrograde action of cannabinoids. *J Neurosci* **25,** 7499-7506.

Melke J, Westberg L, Nilsson S, Landen M, Soderstrom H, Baghaei F, Rosmond R, Holm G, Bjorntorp P, Nilsson LG, Adolfsson R & Eriksson E. (2003). A polymorphism in the serotonin receptor 3A (HTR3A) gene and its association with harm avoidance in women. *Arch Gen Psychiatry* **60,** 1017-1023.

Morales M & Bloom FE. (1997). The 5-HT3 receptor is present in different subpopulations of GABAergic neurons in the rat telencephalon. *J Neurosci* **17,** 3157-3167.

Morales M & Wang SD. (2002). Differential composition of 5-hydroxytryptamine3 receptors synthesized in the rat CNS and peripheral nervous system. *J Neurosci* **22,** 6732-6741.

Moss SJ & Smart TG. (2001). Constructing inhibitory synapses. *Nat Rev Neurosci* **2,** 240-250.

Mossner R, Schmitt A, Hennig T, Benninghoff J, Gerlach M, Riederer P, Deckert J & Lesch KP. (2004). Quantitation of 5HT3 receptors in forebrain of serotonin transporter deficient mice. *J Neural Transm* **111,** 27-35.

Niesler B, Flohr T, Nothen MM, Fischer C, Rietschel M, Franzek E, Albus M, Propping P & Rappold GA. (2001a). Association between the 5' UTR variant C178T of the serotonin receptor gene HTR3A and bipolar affective disorder. *Pharmacogenetics* **11,** 471-475.

Niesler B, Weiss B, Fischer C, Nothen MM, Propping P, Bondy B, Rietschel M, Maier W, Albus M, Franzek E & Rappold GA. (2001b). Serotonin receptor gene HTR3A variants in schizophrenic and bipolar affective patients. *Pharmacogenetics* **11,** 21-27.

Oz M, Ravindran A, Diaz-Ruiz O, Zhang L & Morales M. (2003). The endogenous cannabinoid anandamide inhibits alpha7 nicotinic acetylcholine receptor-mediated responses in Xenopus oocytes. *J Pharmacol Exp Ther* **306,** 1003-1010.

Oz M, Zhang L & Morales M. (2002). Endogenous cannabinoid, anandamide, acts as a noncompetitive inhibitor on 5-HT3 receptor-mediated responses in Xenopus oocytes. *Synapse* **46,** 150-156.

Pacher P, Batkai S & Kunos G. (2006). The endocannabinoid system as an emerging target of pharmacotherapy. *Pharmacol Rev* **58,** 389-462.

Petrini EM, Zacchi P, Barberis A, Mozrzymas JW & Cherubini E. (2003). Declusterization of

GABAA receptors affects the kinetic properties of GABAergic currents in cultured hippocampal neurons. *J Biol Chem* **278,** 16271-16279.

Pratt GD, Bowery NG, Kilpatrick GJ, Leslie RA, Barnes NM, Naylor RJ, Jones BJ, Nelson DR, Palacids JM, Slater P & et al. (1990). Consensus meeting agrees distribution of 5-HT3 receptors in mammalian hindbrain. *Trends Pharmacol Sci* **11,** 135-137.

Sheng M & Pak DT. (2000). Ligand-gated ion channel interactions with cytoskeletal and signaling proteins. *Annu Rev Physiol* **62,** 755-778.

Spier AD, Wotherspoon G, Nayak SV, Nichols RA, Priestley JV & Lummis SC. (1999). Antibodies against the extracellular domain of the 5-HT3 receptor label both native and recombinant receptors. *Brain Res Mol Brain Res* **67,** 221-230.

Spivak CE, Lupica CR & Oz M. (2007). The Endocannabinoid Anandamide Inhibits the Function of {alpha}4{beta}2 Nicotinic Acetylcholine Receptors. *Mol Pharmacol*.

Sun H, Hu XQ, Moradel EM, Weight FF & Zhang L. (2003). Modulation of 5-HT3 receptor-mediated response and trafficking by activation of protein kinase C. *J Biol Chem* **278,** 34150-34157.

Tecott LH, Maricq AV & Julius D. (1993). Nervous system distribution of the serotonin 5-HT3 receptor mRNA. *Proc Natl Acad Sci U S A* **90,** 1430-1434.

van Hooft JA, van der Haar E & Vijverberg HP. (1997). Allosteric potentiation of the 5-HT3 receptor-mediated ion current in N1E-115 neuroblastoma cells by 5-hydroxyindole and analogues. *Neuropharmacology* **36,** 649-653.

Waeber C, Dixon K, Hoyer D & Palacios JM. (1988). Localisation by autoradiography of neuronal 5-HT3 receptors in the mouse CNS. *Eur J Pharmacol* **151,** 351-352.

Waeber C, Hoyer D & Palacios JM. (1989). 5-hydroxytryptamine3 receptors in the human brain: autoradiographic visualization using [3H]ICS 205-930. *Neuroscience* **31,** 393-400.

Waeber C, Pinkus LM & Palacios JM. (1990). The (S)-isomer of [3H]zacopride labels 5-HT3 receptors with high affinity in rat brain. *Eur J Pharmacol* **181,** 283-287.

Yakel JL & Jackson MB. (1988). 5-HT3 receptors mediate rapid responses in cultured hippocampus and a clonal cell line. *Neuron* **1,** 615-621.

Zhang L & Lummis SC. (2006). *5-HT3 receptors*, vol. 522 Pt 2. Marcell Dekker, Inc.

Zimmer A, Zimmer AM, Hohmann AG, Herkenham M & Bonner TI. (1999). Increased mortality, hypoactivity, and hypoalgesia in cannabinoid CB1 receptor knockout mice. *Proc Natl Acad*

Sci U S A **96,** 5780-5785.

Molecular Pharmacology Fast Forward. Published on November 9, 2007 as DOI: 10.1124/mol.107.039149
This article has not been copyedited and formatted. The final version may differ from this version.

Figure Legends

Fig. 1. AEA inhibition of $I_{5\text{-}HT}$ in *Xenopus* oocytes expressing 5-HT_{3A} receptors. A, AEA inhibition of $I_{5\text{-}HT}$. Tracing records showing currents activated by 1 μM 5-HT in the absence and presence of 10 μM AEA. The solid bar on the top of each trace record represents the time of 5-HT application. A long solid bar indicates the time of continuous application of AEA. B, time course of AEA inhibition of $I_{5\text{-}HT}$ in cells previously injected with 2.5 ng cRNA of mouse 5-HT_{3A} subunit. The solid bar indicates the application time of 10 μM AEA. Each data point represents mean ± S.E. from at least 7 oocytes. The error bars that are invisible are smaller than the size of symbols. C, the concentration-response curve of AEA inhibition of $I_{5\text{-}HT}$ in oocytes previously injected with 2.5 ng cRNA of the mouse 5-HT_{3A} subunit. The curve is best fit to the Hill equation as described in 'Methods'. Each data point represents mean ± s. e. from at least 7 oocytes. D, noncompetitive inhibition of 5-HT_{3A} receptor-mediated responses by AEA. 5-HT concentration-response curves in the absence (*open circle*) and in the presence of 10 μM AEA (*solid circle*).

Fig. 2. AEA inhibition depends on expression level of receptor proteins at the cell surface. A, Western blot of 5-HT_{3A} receptor protein at the surface membrane of *Xenopus* oocytes. A representative gel of Western blot showing the abundance of surface proteins from cells previously injected with various concentrations of 5-HT_{3A} receptor cRNAs. B, tracing records showing AEA inhibition of 5-HT-activated currents in cells previously injected with 2.5 ng (*Upper*) and 50 ng (*Lower*) 5-HT_{3A} receptor cRNAs. C, Time course of AEA inhibition of $I_{5\text{-}HT}$ in *Xenopus* oocytes

Molecular Pharmacology Fast Forward. Published on November 9, 2007 as DOI: 10.1124/mol.107.039149
This article has not been copyedited and formatted. The final version may differ from this version.

previously injected with 1, 20 and 50 ng of the 5-HT_{3A} receptor cRNAs. The solid bar indicates the time of AEA application. Each data point represents mean ± s. e. from the average of 5 cells. D, Concentration-response curves of AEA inhibition of 5-HT-activated current in cells previously injected with 1, 2.5 and 50 ng of 5-HT_{3A} receptor cRNAs. The curves were best fit to the Hill equation as described in 'Materials and Methods'. Each data point represents mean ± S.E. from at least 5 oocytes

Fig. 3. AEA inhibition correlates with levels of receptor expression. A, correlation between the magnitude of inhibitory effect induced by 10 μM AEA and various concentrations of 5-HT_{3A} receptor cRNAs injected into oocytes (linear regression, $p < 0.0001$, n = 6). Each data point represents mean ± S.E. from at least 7 oocytes. B, correlation between the magnitude of AEA inhibition and levels of surface 5-HT_{3A} receptor proteins isolated from oocytes previously injected with various concentrations of 5-HT_{3A} receptor cRNA. (Linear regression, $p < 0.001$, n = 5). Each data point represents mean ± S.E. from 3 separate experiments. The band density was normalized as percentage of control. C, correlation between the extent of AEA-induced inhibiting effect on 5-HT_{3A} receptors and current amplitude activated by maximal concentration of 5-HT (100 μM) in oocytes previously injected with 1 ng, 10 ng and 25 ng of 5-HT_{3A} receptor cRNA (Linear regression, $p < 0.01$, n = 24). These data were collected from the same batch of oocytes.

Fig. 4. AcD treatment decreases $I_{5\text{-}HT}$ and increases AEA inhibition of 5-HT_{3A} receptors. A, *bar graphs* of average amplitude of current induced by maximal concentration of 5-HT (100 μM) without and with AcD treatment of *Xenopus* oocytes expressing mouse 5-HT_{3A} receptors. B, *bar*

Molecular Pharmacology Fast Forward. Published on November 9, 2007 as DOI: 10.1124/mol.107.039149
This article has not been copyedited and formatted. The final version may differ from this version.

graphs represent average percentage of AEA inhibition of 5-HT_{3A} receptors without and with AcD treatment. Each data point represents mean ± S.E. from 5 cells. * indicates a significant difference as compared with control ($p < 0.02$).

Fig. 5. AEA inhibition correlates with 5-HT_{3A} receptor density expressed in HEK 293 cells. A, representative current records show low and high density currents induced by 30 μM 5-HT in the absence and presence of 0.1 μM AEA in HEK 293 cells transiently transfected with the cDNA of human 5-HT_{3A} receptors. AEA was pre-applied to a cell for 2 min prior to application of 5-HT. B, correlation between the percent AEA inhibition of current amplitude and MCD (Linear regression, $p < 0.01$, n = 12). C, correlation between the percent AEA inhibition of current area and MCD (Linear regression, $p < 0.01$, n = 12).

Fig. 6. AEA does not alter receptor trafficking. A, imaging of live HEK 293 cells expressing 5-HT_{3A} receptor-BTX in the absence and presence of 2 μM AEA. Alexa 488-BTX was first incubated with a cell before 2 μM AEA in *red*. The cell was labeled with a secondary staining of tetramethylrhodamine-BTX after AEA in *green*. B, a representative Western blot of 5-HT_{3A} receptor surface proteins expressed in *Xenopus* oocytes. C, *bar graphs* represent normalized gel intensity (% of control) of 5-HT_{3A} receptor proteins isolated from cell surface of oocytes in the absence (control) and presence of 2 μM AEA. Each data point represents mean ± S.E. from at least 3 separate experiments.

Fig. 7. AEA accelerates receptor desensitization kinetics. A, tracings of 5-HT-activated currents without and with 0.1 μM AEA recorded from a HEK 293 cell expressing human 5-HT_{3A} receptors.

Molecular Pharmacology Fast Forward. Published on November 9, 2007 as DOI: 10.1124/mol.107.039149
This article has not been copyedited and formatted. The final version may differ from this version.

The amplitude of current in the presence of AEA was normalized. B, the effect of AEA on the time courses of 5-HT-activated current and receptor desensitization. The graph (*solid circles*) plotting average percent 5-HT current amplitude (during AEA incubation) as average percentage of control (amplitude of 5-HT current prior to AEA). The graph (*open circles*) plotting the desensitization time during AEA incubation as average percentage of control (desensitization time before AEA). Each data point represents mean ± S.E. from 5 individual HEK 293 cells. C, *bar graphs* represent the average desensitization time of fast components (left) with and without 0.1 μM AEA. *Bar graphs* (right) represent the sums of fast and slow components of 5-HT_{3A} receptor kinetics without and with AEA. Each data point represents mean ± S.E. from 11 HEK 293 cells. * indicates a significant difference as compared with control ($p < 0.001$).

Fig. 8. Receptor desensitization correlates with MCD and AEA inhibition. A, correlation between 5-HT MCD and receptor desensitization time (Linear regression, $p < 0.01$). B, correlation between average percentage AEA inhibition and receptor desensitization time (Linear regression, $p < 0.01$). C, correlation analysis of 5-HT MCD and receptor activation time (Linear regression, $p = 0.4$). D, correlation analysis of 5-HT MCD and the fast (*solid squares*) and slow (*open squares*) components of receptor deactivation kinetics (Linear regression, $p = 0.5$).

Fig. 9. The effects of NOC and 5-HTID on receptor desensitization and AEA inhibition. A, tracings of 5-HT-activated currents without and with NOC and 5-HTID in HEK 293 cells expressing human 5-HT_{3A} receptors. Cells were pretreated with 25 μM NOC for 4 hrs and washed thoroughly by perfusion solution during the recording. 5-HTID was applied with 5-HT simultaneously. B, the open

Molecular Pharmacology Fast Forward. Published on November 9, 2007 as DOI: 10.1124/mol.107.039149
This article has not been copyedited and formatted. The final version may differ from this version.

bars represent the average percent inhibition induced by 0.1 μM AEA. The solid bars represent average desensitization time with and without 0.1 μM AEA. The average time constant of receptor desensitization is the sum of fast and slow components of 5-HT_{3A} receptor kinetics without and with AEA. Each data point represents mean ± S.E. from 11 cells. * indicates a significant difference as compared with control ($p < 0.02$). ** indicates a significant difference as compared with control ($p < 0.001$). C, bar graphs of the calculated MCD in the absence and presence of NOC and 5-HTID. Each data point represents mean ± S.E. from 14 to 22 cells

Figure 1

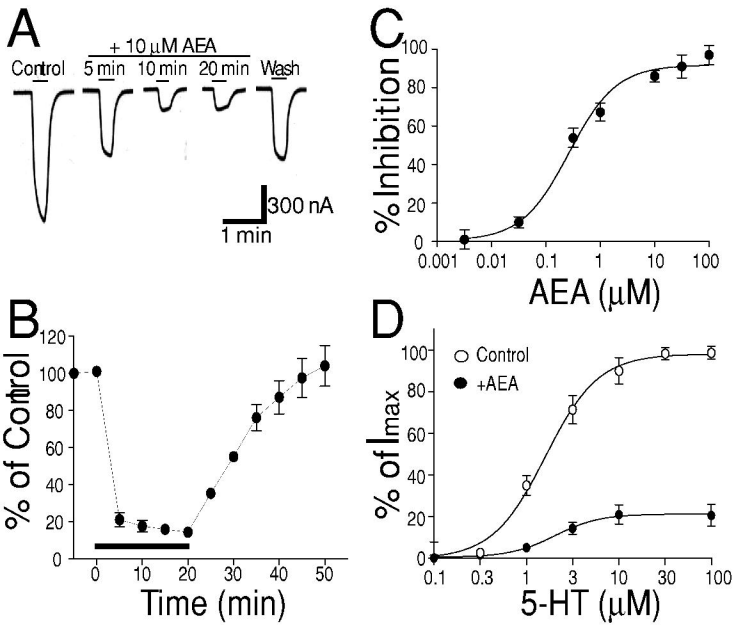
A
+ 10 μM AEA
Control
5 min
10 min
20 min
Wash
300 nA
1 min
B
% of Control
Time (min)
C
% Inhibition
AEA (μM)
D
Control
+AEA
% of Imax
5-HT (μM)

Figure 2

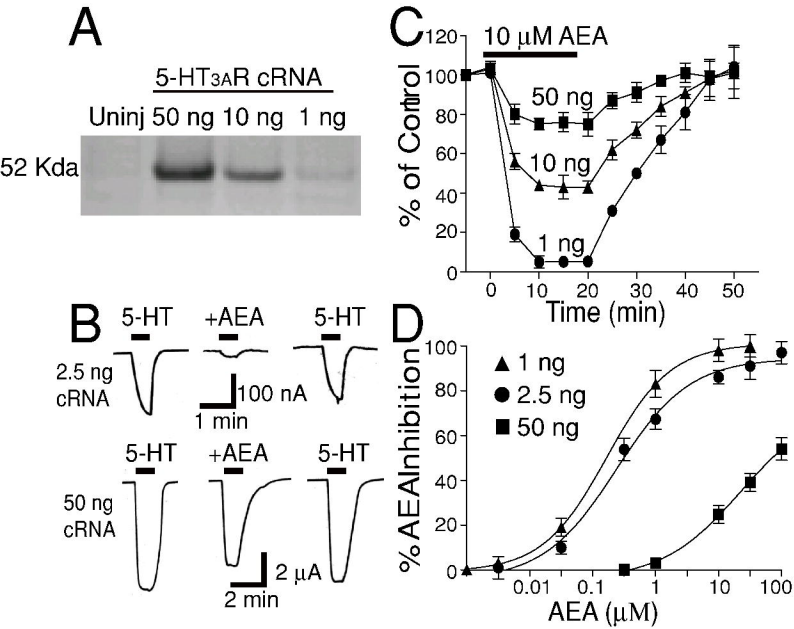
A
5-HT3AR cRNA
Uninj 50 ng 10 ng 1 ng
52 Kda
B
5-HT
+AEA
5-HT
2.5 ng cRNA
100 nA
1 min
5-HT
+AEA
5-HT
50 ng cRNA
2 µA
2 min
C
10 µM AEA
% of Control
50 ng
10 ng
1 ng
Time (min)
D
%AEAInhibition
1 ng
2.5 ng
50 ng
AEA (µM)

Figure 3

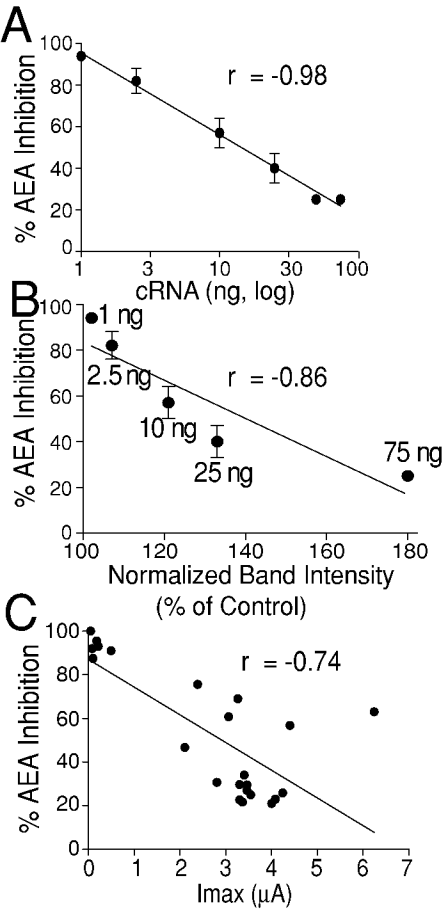
A
% AEA Inhibition
r = -0.98
cRNA (ng, log)
B
% AEA Inhibition
1 ng
2.5 ng
10 ng
25 ng
75 ng
r = -0.86
Normalized Band Intensity
(% of Control)
C
% AEA Inhibition
r = -0.74
Imax (μA)

Figure 4

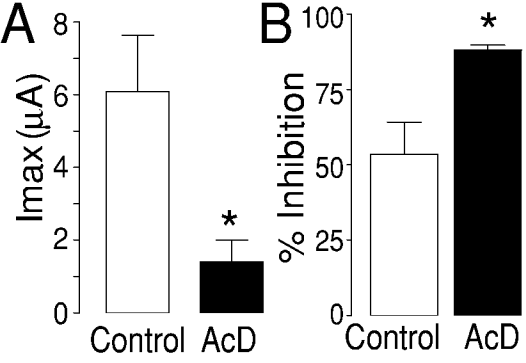
A
Imax (μA)
8
6
4
2
0
*
Control
AcD
B
% Inhibition
100
75
50
25
0
*
Control
AcD

Figure 5

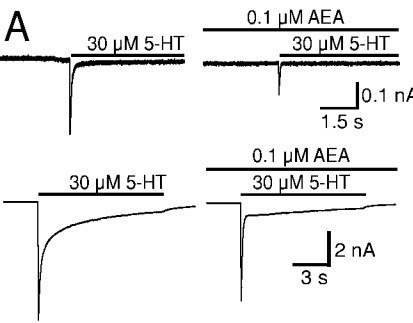
A
30 μM 5-HT
0.1 μM AEA
30 μM 5-HT
0.1 nA
1.5 s
30 μM 5-HT
0.1 μM AEA
30 μM 5-HT
2 nA
3 s

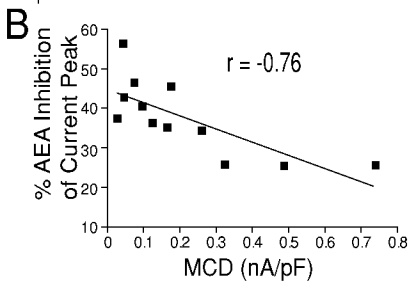
B
% AEA Inhibition of Current Peak
r = -0.76
MCD (nA/pF)

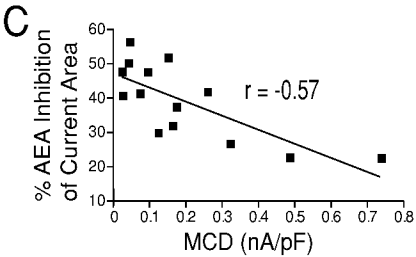
C
% AEA Inhibition of Current Area
r = -0.57
MCD (nA/pF)

Figure 6

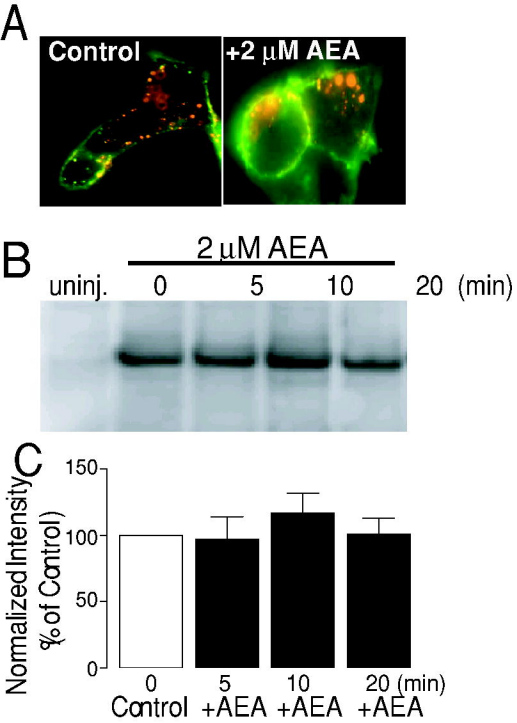
A
Control
+2 μM AEA
B
2 μM AEA
uninj.
0
5
10
20 (min)
C
Normalized Intensity
(% of Control)
150
100
50
0
0
5
10
20 (min)
Control
+AEA
+AEA
+AEA

Figure 7

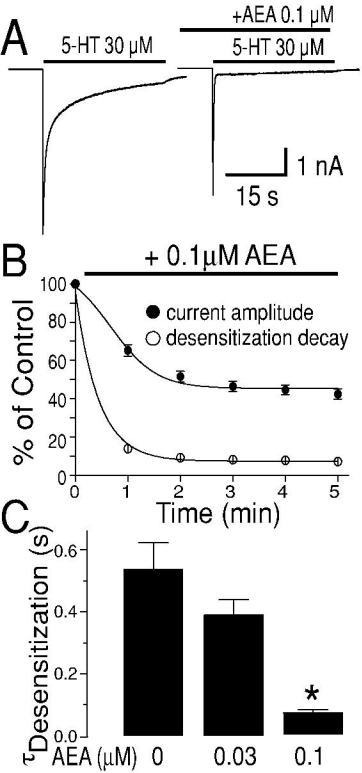
A
5-HT 30 µM
+AEA 0.1 µM
5-HT 30 µM
1 nA
15 s
B
+ 0.1µM AEA
% of Control
current amplitude
desensitization decay
Time (min)
C
τDesensitization (s)
AEA (µM) 0
0.03
0.1
*

Figure 8

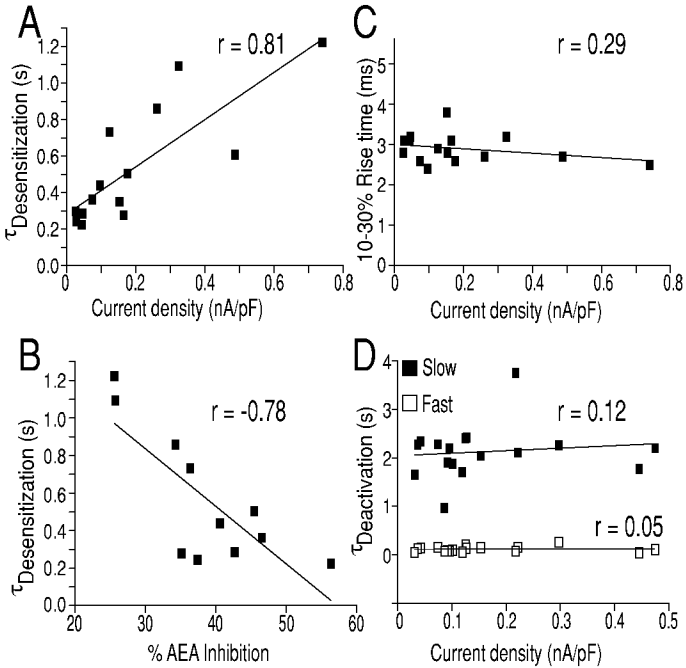
A
r = 0.81
τDesensitization (s)
Current density (nA/pF)
C
r = 0.29
10-30% Rise time (ms)
Current density (nA/pF)
B
r = -0.78
τDesensitization (s)
% AEA Inhibition
D
Slow
Fast
r = 0.12
r = 0.05
τDeactivation (s)
Current density (nA/pF)

Figure 9

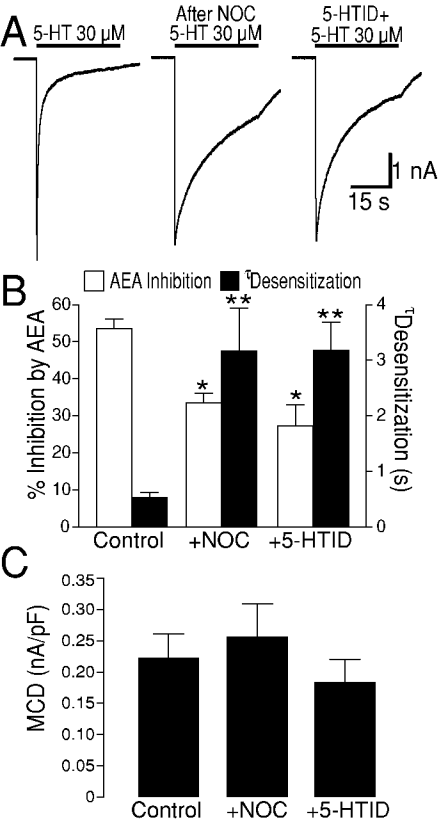
A
5-HT 30 µM
After NOC
5-HT 30 µM
5-HTID+
5-HT 30 µM
1 nA
15 s
B
AEA Inhibition
τDesensitization
% Inhibition by AEA
τDesensitization (s)
Control
+NOC
+5-HTID
C
MCD (nA/pF)
Control
+NOC
+5-HTID